n-p Triple Scattering Parameter R_t at 203 MeV*

N. W. REAY, E. H. THORNDIKE, D. SPALDING, AND A. R. THOMAS
Department of Physics and Astronomy, University of Rochester, Rochester, New York

(Received 25 April 1966)

The neutron-proton interaction has been studied by bombarding deuterons with 203-MeV polarized protons and observing high-energy neutrons recoiling into forward angles. The triple-scattering parameter R_t was measured at neutron laboratory angles between 0° and 20°, using a spin-analyzing scatterer of liquid hydrogen, and detecting charge-exchange scattered protons therefrom. The measurements are related to the free n-p scattering amplitudes by means of an impulse-approximation calculation which includes the s-wave final-state interaction between the incident proton and the proton in the deuteron. The measured values of R_t are compared with the phase-shift solutions YLAN of Breit and collaborators, and the energy-independent solution of Arndt and MacGregor. Solutions YLAN 0, 1, 2, $2M$, and 3 do *not* agree with the date. Solutions YLAN 3M and 4M and the Arndt-MacGregor solution fit the data quite well.

I. INTRODUCTION

We have studied the neutron-proton interaction[1] by bombarding a liquid-deuterium target with 207-MeV polarized protons from the University of Rochester 130-in. synchrocyclotron and observing high-energy neutrons recoiling into forward angles. A measurement of the polarization parameter P is reported in the following article,[2] while this article is devoted to the triple-scattering parameter R_t.

The sub-t triple-scattering parameters differ from the conventional quantities, because the target particle is spin analyzed, instead of the incident particle; that is, the polarization transferred between the particles is investigated. R_t is defined by

$$\langle \boldsymbol{\sigma}_b \rangle_f \cdot \mathbf{s}_t = R_t [\langle \boldsymbol{\sigma}_a \rangle_i \cdot (\mathbf{n}_t \times \mathbf{k})]. \quad (1)$$

$\langle \boldsymbol{\sigma}_b \rangle_f$ is the final polarization of the target particle, $\langle \boldsymbol{\sigma}_a \rangle_i$ is the initial polarization of the incident particle, $\mathbf{s}_t$, $\mathbf{n}_t$, and $\mathbf{k}$ are unit vectors shown in Fig. 1, a denotes the incident particle, and b the target particle. Equation (1) assumes that the target is unpolarized ($\langle \boldsymbol{\sigma}_b \rangle_i = 0$) and the incident beam has components of polarization only in the $(\mathbf{n}_t \times \mathbf{k})$ direction

$$\langle \boldsymbol{\sigma}_a \rangle_i \cdot \mathbf{n}_t = 0 = \langle \boldsymbol{\sigma}_a \rangle_i \cdot \mathbf{k}.$$

The following section describes the impulse-approximation calculation used to relate our measurements to the n-p interaction. Section III contains the experimental details, while the results are presented and compared with phase-shift information in Sec. IV.

II. THEORY

The conventional way of relating p-d scattering to nucleon-nucleon scattering is by means of the impulse approximation.[3] Quasifree p-p scattering data are described qualitatively by the simple spectator model[4] with no final-state interactions (FSI); however, if s-wave final-state interactions are included,[5] the agreement between experiment and theory is much improved. "Slightly inelastic" p-d scattering[6] is also fitted satisfactorily by an impulse-approximation calculation with s-wave FSI.[7] Such a theory is believed to be sufficiently accurate for our purposes.

Cromer[7] has calculated "slightly inelastic" proton-deuteron scattering $[p+d \to p+(n+p)]$ where the first proton emerges into small angles with high energy. We have followed his calculation making the necessary changes to describe the reaction $p+d \to n+(p+p)$ with a high-energy *neutron* emerging into small angles. The calculation is intuitively described as follows: A proton (plane wave) is incident on a deuteron (triplet-spin ground-state wave function), the incident proton and target neutron interact (M_{np}, the free n-p scattering matrix) with the neutron, recoiling into small angles (plane wave) and with the two protons emerging with

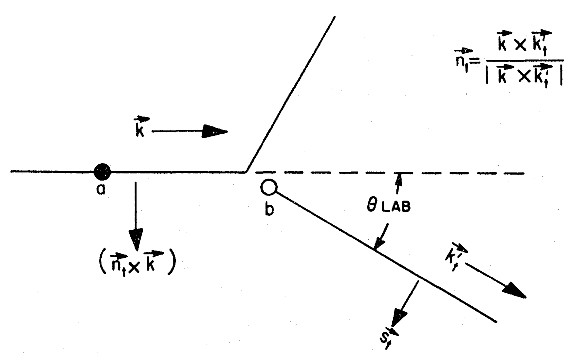

FIG. 1. A scattering event, viewed in the laboratory system, showing the unit vectors $\mathbf{k}$, $\mathbf{k}_t$, $\mathbf{s}_t$, and $\mathbf{n}_t$.

* Supported by the U. S. Atomic Energy Commission.
[1] Recent reviews on this subject have been written by Wilson [R. Wilson, *The Nucleon-Nucleon Interaction* (Interscience Publishers, Inc., New York, 1963)] and by Moravcsik [M. J. Moravcsik, *The Two-Nucleon Interaction* (Clarendon Press, Oxford, England, 1963)].
[2] D. Spalding, A. R. Thomas, N. W. Reay, and E. H. Thorndike, following paper, Phys. Rev. **150**, 806 (1966).
[3] G. F. Chew, Phys. Rev. **80**, 196 (1950).
[4] A. Kuckes, R. Wilson, and P. Cooper, Ann. Phys. (N. Y.) **15**, 193 (1961).
[5] A. H. Cromer and E. H. Thorndike, Phys. Rev. **131**, 1680 (1963).
[6] D. G. Stairs, R. Wilson, and P. F. Cooper, Jr., Phys. Rev. **129**, 1672 (1963).
[7] A. H. Cromer, Phys. Rev. **129**, 1680 (1963).

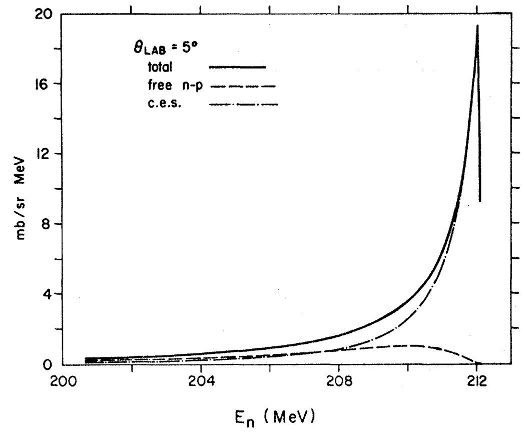

FIG. 2. Predicted neutron spectrum at 5°. The dashed curve is the "free-n-p" contribution [the first term on the right-hand side of Eq. (2)]; the dot-dash curve is the "charge-exchange singlet" contribution [the second term on the right-hand side of Eq. (2)]. The solid curve is their sum, the calculated cross section.

relative momentum k ($\psi_{pp}(k)$). $\psi_{pp}(k)$, the p-p continuum wave function, is spacewise antisymmetric for the triplet spin state and symmetric for the singlet spin state. All states in $\psi_{pp}(k)$, except the s state, are described by a plane wave, while the s-wave FSI is included by using a square-well potential with parameters chosen to fit the effective range and scattering length. Coulomb effects are ignored.

We obtain

$$R_t(E_n)(d^2\sigma/d\Omega_n dE_n)=a(E_n)I_0{}^{np}R_t{}^{np}+2b(E_n)I_0{}^{\text{ces}}R_t{}^{\text{ces}}. \quad (2)$$

Cromer's equation for a scattered *proton* is

$$R(E_p)(d^2\sigma/d\Omega_p dE_p)=a(E_p)[I_0{}^{np}R^{np}+I_0{}^{pp}R^{pp}]+b(E_p)I_0{}^sR^s+c(E_p)I_0{}^tR^t. \quad (3)$$

In these expressions, any quantity other than R_t is obtained by replacing $R_t{}^{np}$, $R_t{}^{\text{ces}}$, etc., by the comparable desired quantity. In particular, the cross section is obtained by replacing $R_t{}^{np}$ and $R_t{}^{\text{ces}}$ by 1.

The coefficients a, b, c are form-factor–like quantities evaluated by Cromer.[7] $I_0{}^{np}$, R^{np}, $I_0{}^{pp}$, and R^{pp} are the free np and pp differential cross sections and R parameters, while $I_0{}^s$, R^s, $I_0{}^t$, and R^t are the singlet and triplet cross sections and R parameters. As defined by Cromer,[5,7] $I_0{}^s=\frac{1}{3}\Sigma_s$, $I_0{}^t=\Sigma_t$. Ces refers to charge-exchange singlet; the ces parameters are obtained from the scattering matrix $M^{\text{ces}}=\Lambda^s(1,3)M_{np}(1,2)\Lambda^t(2,3)$, where Λ^s and Λ^t are singlet and triplet spin-projection operators and M_{np} is the free-np scattering matrix. That is, proton (1) is incident on a neutron (2) and proton (3) bound in a triplet spin state, the neutron and proton (1) interact with the neutron being observed, with the two protons being left in a singlet spin state. Charge independence implies the equality of singlet and charge-exchange singlet cross sections, R parameters, and so on. Comparing our result [Eq. (2)] to Cromer's result [Eq. (3)] we note that antisymmetrization has increased the singlet term by a factor of 2 and eliminated the triplet term. Also, since we observe the recoil target neutron, $\theta_{\text{c.m.}}\approx\pi-2\theta_{\text{lab}}$, rather than $2\theta_{\text{lab}}$. In Table I, the various quantities in Eq. (2) are related to the np scattering matrix.

TABLE I. Expressions for charge-exchange singlet and free-n-p scattering parameters.

$$M_{np}(1,2)=A_{np}+B_{np}\sigma_{1n}\sigma_{2n}+C_{np}(\sigma_{1n}+\sigma_{2n})+E_{np}\sigma_{1q}\sigma_{2q}+F_{np}\sigma_{1p}\sigma_{2p}{}^{\text{a}}$$
$$\alpha=\tfrac{1}{4}[3A_{np}-B_{np}-E_{np}-F_{np}]$$
$$\beta=\tfrac{1}{4}[A_{np}-3B_{np}+E_{np}+F_{np}]$$
$$\gamma=\tfrac{1}{4}[A_{np}+B_{np}+E_{np}-3F_{np}]$$
$$\delta=\tfrac{1}{4}[A_{np}+B_{np}-3E_{np}+F_{np}]$$

$$I_0{}^{\text{ces}}=\tfrac{1}{3}\{|\alpha|^2+|\beta|^2+|\gamma|^2+|\delta|^2+|C_{np}|^2\}$$
$$I_0P^{\text{ces}}=\tfrac{1}{3}\{2\,\text{Re}[C_{np}{}^*(\alpha-\beta)]\}$$
$$I_0D_t{}^{\text{ces}}=\tfrac{1}{3}\{2\,\text{Re}[\gamma^*\delta-\alpha^*\beta]+|C_{np}|^2\}$$
$$I_0(x-y)^{\text{ces}}=\tfrac{1}{3}\{2\,\text{Re}[\beta^*\delta-\alpha^*\gamma]+|C_{np}|^2\}$$
$$I_0Z^{\text{ces}}=-\tfrac{1}{3}\{2\,\text{Im}[C_{np}{}^*(\alpha-\beta)]\}$$
$$R_t{}^{\text{ces}}=(x-y)^{\text{ces}}\cos(\theta^n{}_{\text{lab}})-Z^{\text{ces}}\sin(\theta^n{}_{\text{lab}})$$
$$I_0{}^{np}=|A_{np}|^2+|B_{np}|^2+2|C_{np}|^2+|E_{np}|^2+|F_{np}|^2$$
$$I_0D_t{}^{np}=2(\text{Re}AB^*+\text{Re}EF^*+|C|^2)$$
$$I_0K_{qp}{}^{np}=-2\,\text{Im}[C^*(E+F)]$$
$$I_0K_{pp}{}^{np}=2(\text{Re}AF^*+\text{Re}BE^*)$$
$$R_t{}^{np}=K_{qp}{}^{np}\sin\theta^n{}_{\text{lab}}+K_{pp}{}^{np}\cos\theta^n{}_{\text{lab}}$$

[a] **n**, **p**, **q** are the *conventional* unit vectors, defined by the *scattered* particle, rather than the target particle.

The predicted neutron spectra for 5° and 20° lab are shown in Figs. 2 and 3. At 5° singlet scattering dominates and is sharply peaked. At 20° the broader peak of the free-n-p scattering is dominant.

III. THE EXPERIMENT

The experimental layout is shown in Fig. 4. The 207-MeV proton beam, initially 90% polarized in the vertical direction, passes through a 7-ft long solenoid (S), which can precess the polarization[1] by 90° about its axis (the magnetic field direction) for a given setting of the solenoid current designated by N (normal). If the

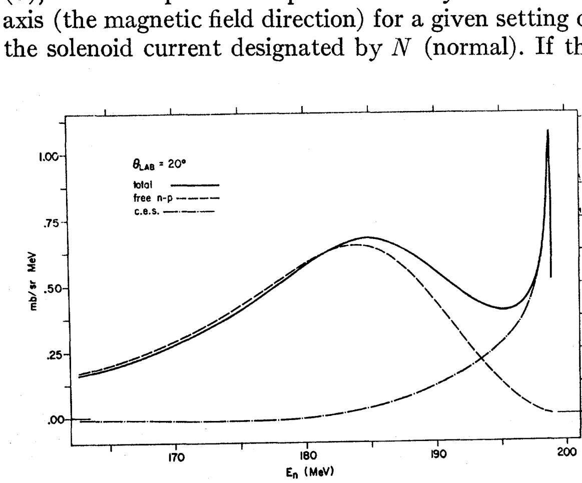

FIG. 3. Predicted neutron spectrum at 20°. The curves are as in Fig. 2.

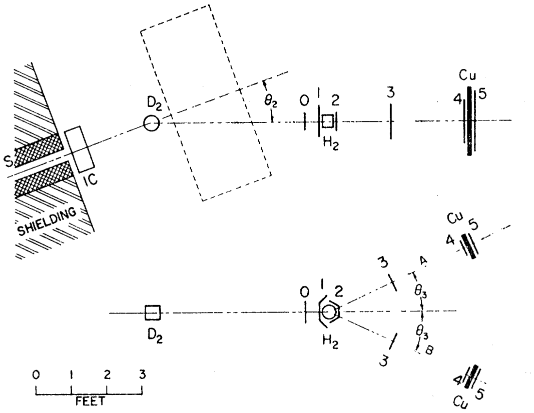

FIG. 4. Plan and elevation views of the experimental layout, showing the solenoid magnet (S), ion chamber (IC), deuterium target (D_2), hydrogen target (H_2), scintillation counters 0—5, and absorber (Cu). The position of the wide-gap magnet, used for the 0° measurement, is shown by the dashed rectangle in the plan view.

direction of the current in the solenoid is reversed (designated by R), the polarization precesses again by 90°, but in the opposite direction, giving a total difference of 180° in the polarization direction for solenoid current N to R. The beam emerging from the solenoid with horizontal polarization passes through an ion-chamber (IC) beam-intensity monitor and strikes a deuterium target (D_2) 5 in. high×5 in. in diameter, and with 0.003-in. beryllium-copper walls. The beam size at the deuterium target is typically 4-in. high×$1\frac{1}{2}$-in. wide.

After charge-exchange scattering in the deuterium target, neutrons recoiling at angle θ_2 in the horizontal plane pass through the anticoincidence counters 0, 1 onto a liquid-hydrogen target (H_2) of 0.005-in. Mylar, 5 in. in diameter×4-in. long. (The designation 0 is sometimes omitted.) By measuring the asymmetry of neutron-scattered protons recoiling into angle θ_3^{lab} $(=25°)$ in the vertical plane, the neutron polarization is determined. The protons are detected by two identical telescopes (A and B), consisting of two counters (3,4), some copper absorber (Cu), and a final counter (5). Thus, the complete logic requirement for detecting a neutron from the deuterium target is $\bar{0}\bar{1}2(345A)$ or $\bar{0}\bar{1}2(345B)$. The telescopes are physically interchangeable, occupying either θ_3 up (U) or down (D) positions.

If I_{km} is the counting rate for a θ_3^{lab} direction $k(=U$ or $D)$ and solenoid current direction $m(=N$ or $R)$, then the asymmetry in the hydrogen scattering, e_{3s}, is given by

$$e_{3s}=(I_{DN}+I_{UR}-I_{UN}-I_{DR})/(I_{DN}+I_{UR}+I_{UN}+I_{DR})\,. \tag{4}$$

From e_{3s} we can get the desired parameter R_t by

$$e_{3s}=R_tP_1P_3\,, \tag{5}$$

where P_1 is the polarization of the initial proton beam and P_3 is the analyzing power of the n-p scattering in the hydrogen.

The polarization reversal of the solenoid and the physical interchangeability of the A and B telescopes causes the cancellation of all first-order errors to Eq. (5), except those due to beam movement caused by reversal of the solenoid magnetic field. Vertical-beam profiles at the deuterium-target entrance were measured frequently to detect beam movement and a first-order correction to e_{3s} varying from 0.0000 ± 0.0008 to 0.0008 ± 0.0015 was applied to the data.

Deuterium-target empty backgrounds varied from 6% to 11% of the target full rate, while the only serious random-coincidence rate, $\bar{0}\bar{1}2$ in random coincidence with 345, was $\frac{1}{2}$% to $7\frac{1}{2}$% of the true rate and was monitored simultaneously in data runs. The inefficiency of the anticoincidence counters causing charged particles to be recorded $\bar{0}\bar{1}$ 2345 events varied from $\frac{1}{2}$% to 3% of the total $\bar{0}\bar{1}$ 2345 rate. We corrected the asymmetry for the above three sources of background and included an additional error, allowing for systematic inaccuracies in the corrections. The dominant error was still due to counting statistics. Table III shows e_{3s} plus its error.

The analyzing power P_3 is taken as the free n-p scattering polarization parameter P_{np} at the recoil-proton angle of 25° lab. We have *not* corrected for hydrogen-target empty "background." Such "background," a 25% effect, is predominantly due to (n,p) reactions in the carbon of the scintillation counters 1 and 2. The following article[2] shows that the analyzing power of (n,p) reactions in carbon is essentially equal to P_{np}, and hence we can consider such counts as useful data rather than background.

If E_3 is the energy of the analyzing scattering, then we can write

$$P_3(E)\approx P_{np}(210\text{ MeV})+(\partial P_{np}/\partial E)\times(E_3-210\text{ MeV})\,. \tag{6}$$

From existing data and phase-shift analyses, we find that $P_{np}(210)=0.13\pm0.02$ and $\partial P_{np}/\partial E=(0.0012\pm0.0002)/\text{MeV}$. $\bar{E}_3$, the mean energy of the analyzing scattering, has been obtained in two ways. (1) The energy spectrum of the primary beam and the theoretically-predicted spectrum of scattered neutrons have been folded together and weighted by a calculated neutron-detection efficiency to obtain the mean energy. (2) Range curves, taken by varying the absorber in the 345 telescope, have been "traced back" to give $\bar{E}_3$. The agreement between the two methods is satisfactory. The combined result is shown in Table III. The errors shown cover any disagreement between the two methods.

At small angles (0° and 5° lab), the incident proton beam passing through the deuterium target strikes directly the analyzing target and the 0, 1, 2 counters, causing a violent increase in the counting rate and making efficient separation of neutrons impossible. To prevent this, a wide-gap magnet was installed downstream of the deuterium target (see Fig. 4) to deflect the proton beam by 6°. Further, a compact polyethylene target was used instead of a liquid-hydrogen target and the sizes of the 0, 1, 2 counters were correspondingly reduced.

To minimize the number of deuterium-produced neutrons that scattered from the magnet into the analyzing target, material near the beam line was minimized. The magnet pole tips were 16 in. along the beam and 6 in. across the beam, with the gap between pole tips of 20 in. All other material was 20 in. away from the beam line. The scattering from this magnet was calculated to be $\gtrsim 0.5\%$. To check the effect of the magnet, the 5° point was measured with and without the magnet and shows agreement to 0.08 ± 0.15 in R_t. At 0°, an error in R_t of 0.01 is included, to allow for magnet scattering.

The polarization of the neutrons precesses through 14° in the magnetic clearing field, reducing the R_t parameter and mixing in the R'_t parameter. The corrections to R_t for this effect were 0.008 at 0° and 0.018 at 5°.

IV. RESULTS

The conditions of each measurement are shown in Table II. At 10° and 15°, measurements were made on both sides (north and south) of the direct-beam line, while at 5° and 20°, measurements were only made on the north side, as shown in Fig. 4. The first column indicates the intended laboratory angle of the recoiling neutron, with N and S indicating the side. The third column shows the actual laboratory angle of the recoiling neutron. The primary-beam energy was determined from range curves taken with copper, using the range-energy relations of Rich and Madey.[8] The mean energy at the center of the deuterium target is shown in the table. The energy spread due to the primary beam and the finite target size was 12 MeV, full width at half-maximum. The angular resolution in the laboratory scattering angle θ_2 was $\pm 1°$ (rms), corresponding to a center-of-mass angular resolution of $\pm 2°$ (rms). The equivalent n-p center-of-mass scattering angle, shown in the fourth column, is defined as that corresponding to the same momentum transfers as the p-d event.

TABLE II. Experimental conditions for each measurement: mean scattering energy, laboratory scattering angle, equivalent two-nucleon center-of-mass scattering angle, and E_b and E_u, energies relevant to the neutron-detection efficiency.

Nominal angle	Mean energy (MeV)	θ_2 (deg)	$\theta_{\text{c.m.}}$ (deg)	E_b (MeV)	E_u (MeV)
0°	198.5±2.0	0.35±0.3	179.2±0.6	170	183
5°N	198.5±2.0	5.15±0.3	169.2±0.6	170	183
10°N	211.8±1.0	10.0 ±0.3	158.9±0.6	164	178
10°S	209.0±1.0	10.0 ±0.3	158.9±0.6	175	189
15°N	202.0±4.0	14.6 ±0.4	149.2±0.8	153	167
15°S	209.0±1.0	15.0 ±0.3	148.4±0.6	164	178
20°N	202.0±4.0	19.5 ±0.4	139.0±0.8	140	151

The detection efficiency of the hydrogen scatterer depended on the energy of the neutrons incident on it. This dependence was investigated by a computer program, which assumed that the contribution of counts from carbon had the same dependence as counts from hydrogen. To fair accuracy, the efficiency can be taken as zero below some neutron energy E_b and rising linearly with energy to E_u, then falling slowly as the np charge-exchange laboratory cross section (at 25°lab) $\sigma_{\text{c.e.}}(E_n,25°)$ above E_u. E_b and E_u, which depend on the absorber used in the 345 telescope, are listed in the last two columns of Table II.

The results of each measurement are shown in Table III. E_3, the mean neutron energy incident upon the third scatterer, is used to obtain P_3 and analyzing power, from Eq. (6). The uncertainties in P_3 due to the uncertainty in $P_{np}(210\text{ MeV})$, $\partial P_{np}/\partial E$, and E_3, are also shown. The measurement at $\theta_2=20°N$ was performed with $\theta_3=20.7°$ lab, because of an oversight in alignment. P_3 has been corrected for this difference in θ_3 and the uncertainty in this correction is given. e_{3s}, with its error, is shown in the last column.

TABLE III. Results of each measurement: mean energy of the third or analyzing scattering, the analyzing power P_3 and errors to it from various sources, and the asymmetry e_{3s} with its error.

Nominal angle	E_3 (MeV)	P_3	Errors to P_3 $\delta(P_3(210))$	$\delta(\partial P_3/\partial E_3)$	$\delta(\Delta E_3)$	Asymmetry
0°	194±3	0.111	±0.020	±0.003	±0.004	−0.0262±0.0091
5°N	194±3	0.111	±0.020	±0.003	±0.004	−0.0540±0.0095
10°N	$197\frac{1}{2}\pm3\frac{1}{2}$	0.115	±0.020	±0.003	±0.004	−0.1027±0.0096
10°S	200±3	0.118	±0.020	±0.002	±0.004	−0.0919±0.0099
15°N	183±4	0.097	±0.020	±0.005	±0.005	−0.0863±0.0069
15°S	$190\pm3\frac{1}{2}$	0.106	±0.020	±0.004	±0.004	−0.0875±0.0065
20°N[a]	$171\frac{1}{2}\pm3\frac{1}{2}$	0.095	±0.020	±0.008	±0.004	−0.0519±0.0100

[a] The scattering angle θ_3 was 20.7° lab for this measurement, rather than 25°. An error to P_3 of ±0.005 results from the uncertainty in the correction for the different angle.

[8] M. Rich and R. Madey, University of California Radiation Laboratory Report No. UCRL-2301 (unpublished).

TABLE IV. R_t and errors in it from various sources. Also given are numbers relevant to the division of R_t between "free np" and "charge-exchange singlet" scattering.

Nominal angle	R_t	Errors in R_t: δ (asymmetry)	$\delta(P_3(210))$	$\delta(\partial P_3/\partial E_3)$	$\delta(\Delta E_3)$	$\delta(P_1)$	a/b	$I_0^{np}/2I_0^s$	$aI_0^{np}/2bI_0^s$
0°	−0.269	±0.094	±0.048	±0.007	±0.010	±0.009	0.01	1.53	0.015
5°N	−0.540	±0.095	±0.097	±0.015	±0.019	±0.018	0.19	1.56	0.30
10°N	−0.992	±0.093	±0.173	±0.022	±0.035	±0.033	0.73	1.56	1.14
10°S	−0.865	±0.093	±0.146	±0.015	±0.026	±0.029	0.67	1.56	1.04
15°N	−0.989	±0.079	±0.197	±0.049	±0.049	±0.032	1.70	1.56	2.66
15°S	−0.917	±0.068	±0.173	±0.035	±0.036	±0.031	1.50	1.56	2.35
20°N[a]	−0.607	±0.117	±0.127	±0.051	±0.025	±0.020	3.87	1.55	6.00

[a] An error in R_t of ±0.032 results from the uncertainty in P_3 mentioned in the footnote to Table III.

R_t is obtained from e_{3s} and P_3 by Eq. (5), taking[9] P_1 as 0.90±0.03. R_t and errors to it from e_{3s}, P_3, and P_1 are shown in Table IV. The errors from δ (asymmetry) and from $\delta(\Delta E_3)$ are random, while errors from $\delta(P_3(210\text{ MeV}))$, $\delta(\partial P_3/\partial E_3)$, and δP_1 are systematic over all angles measured; i.e., all values of R_t move up and down together. Note the agreement between the pairs of measurements at 10° and 15°.

The measured value of R_t is a combination of R_t^{np} and R_t^{ces}, as shown in Eq. (2). This equation has been multiplied by the neutron-detection efficiency and integrated over neutron energy to obtain the mean values of $a(E_n)$ and $b(E_n)$. The ratio of these mean values (a/b) is shown in Table IV. Taking I_0^{np} and I_0^{ces} from phase-shift solution YLAN-3M of Breit and collaborators,[10] the ratio $I_0^{np}/2I_0^{ces}$ is also listed. The product of a/b and $I_0^{np}/2I_0^{ces}$ gives the ratio of events from free-n-p and charge-exchange singlet scattering. This product is listed in the last column of Table IV.

For many purposes, a simpler presentation of results than that given in Tables II and IV is adequate. Such a presentation appears in Table V, which averages measurements at N and S angles. All errors listed in Table IV are combined into the random error listed in Table V, as well as a systematic error which moves all values of R_t together by ±20% of their value. The mean energy of the scattering is 203 MeV.

TABLE V. Simplified summary of R_t results. In addition to the errors listed, which are largely random, there is a systematic error which moves all values of R_t by ±20% of their value. The last column is the ratio of "free np" to "charge-exchange singlet" scattering.

$\theta_{c.m.}$ (deg)	R_t	$aI_0^{np}/2bI_0^s$
179.2	−0.269±0.095	0.015
169.2	−0.540±0.096	0.30
158.9	−0.929±0.070	1.09
148.8	−0.953±0.061	2.50
139.0	−0.607±0.124	6.00

The results, as presented in Table V, are plotted in Fig. 5. In addition to the error bars shown, all values of R_t may move up or down together by ±20%. The curves shown in the figure are results of calculations following the procedure outlined two paragraphs above, and using an assortment of phase-shift solutions to obtain the values of R_t^{np} and R_t^{ces}.

The curve labelled A-M uses the recent energy-independent solution of the Livermore group,[11] and adequately fits the data. The other curves are based on the original YLAN solutions (1,3,3M) of Breit and collaborators,[10] and the most recent extension[12] of that work, (4M). Of the six original YLAN solutions, only YLAN-3M adequately fits the data. This solution was the one preferred by Breit and collaborators.[10] Solution 4M also fits satisfactorily. Solutions 0, 2, and 2M (not

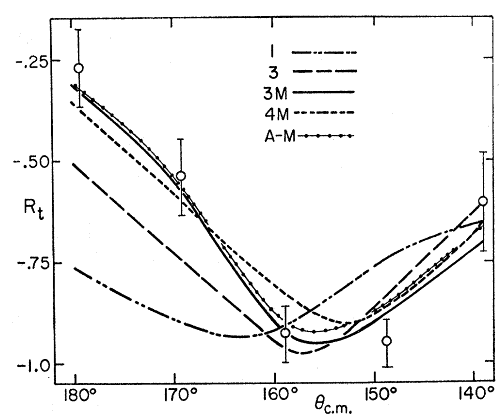

FIG. 5. Plot of the R_t parameter versus the two-nucleon center-of-mass scattering angle. The curves are calculations based on phase-shift solutions YLAN 1, 3, 3M, 4M of Breit and collaborators (Refs. 9, 11) and on the energy-independent solution of Arndt and MacGregor (Ref. 10).

[9] The beam polarization was not measured in this experiment, but was inferred from other recent determinations at this laboratory, all of which depend on the p-carbon polarization measurements of W. G. Chestnut, E. M. Hafner, and A. Roberts, Phys. Rev. **104**, 449 (1956).

[10] M. Hull, K. Lassila, H. Ruppel, F. McDonald, and G. Breit, Phys. Rev. **122**, 1606 (1961).

[11] R. A. Arndt and M. MacGregor, Phys. Rev. **141**, 873 (1966).

[12] G. Breit, R. E. Seamon, and R. D. Haracz (private communication).

shown) are worse fits than solution one. The χ^2 values for solutions 3M, 4M, A-M, and 3 (the closest bad fit) are 2.5, 5.8, 3.6, and 15.6, respectively. The expected value for a reasonable fit is five, the number of data points.

Solutions 3M, 4M, and A-M also give quite acceptable fits to the polarization measurements reported in the following paper.[2] Since our R_t and P data were *not* used as input for any of the phase-shift searches, the good agreement suggests that 3M, 4M, and A-M are fairly close to the true solutions near 203 MeV, and further changes in them in this energy region will be small.

ACKNOWLEDGMENTS

We wish to thank Dr. R. Wright, Professor G. Breit, and Professor P. Signell for helpful communications concerning phase-shift analyses. We are grateful to Professor Alan Cromer for discussions about our impulse-approximation calculation, and for numerical evaluations of the needed coefficients. P. Koehler and L. Moyer assisted with various aspects of the experiment. S. Chadwick, D. Harmon, and M. Eipper helped with data reduction. The experiment depended heavily upon the various support groups of the 130-Inch Cyclotron Laboratory: cyclotron operating crew, mechanical design group, machine shop, and electronics shop.

PHYSICAL REVIEW VOLUME 150, NUMBER 3 21 OCTOBER 1966

Asymmetry in the (p,n) Reaction on Deuterium and Carbon at 215 MeV*†

D. Spalding, A. R. Thomas, N. W. Reay, and E. H. Thorndike
University of Rochester, Rochester, New York
(Received 25 April 1966)

A double-scattering experiment was performed on targets of deuterium and carbon, using 215-MeV, 85% polarized protons as incident particles. The asymmetry of recoil neutrons was measured at laboratory angles between 10° and 35°, using a neutron counter consisting of a polyethylene converter and multi-element scintillation telescope. The deuterium measurements are related to the free n-p polarization parameter by an impulse-approximation calculation. The deuterium results are in good agreement with the predictions of Yale phase-shift solutions 3, 3M, and 4M and the new Livermore solution, and are incompatible with Yale solutions 0, 1, 2, 2M. The asymmetries from carbon agree with free-n-p scattering except at laboratory angles of 10° and 35°, where they are greater in absolute value. The asymmetry from carbon showed the greatest dependence on neutron energy at these angles.

I. INTRODUCTION

We have measured the asymmetry parameter P in the (p,n) reaction on deuterium and carbon targets.

The p-d scattering can be related to free nucleon-nucleon scattering by making the impulse approximation. A calculation appropriate to the final state occurring in the present measurements is described in the preceding paper.[1] Using this calculation, we can compare the predictions of various phase-shift solutions against our measurements.

We have studied the (p,n) reactions on carbon principally to allow use of the charge-symmetric (n,p) reaction in neutron-spin analysis. For example, in Ref. 1 neutron spin was analyzed by hydrogen associated with considerable carbon contaminant. The similarity of asymmetry parameters for carbon and hydrogen (demonstrated in this experiment) makes a carbon subtraction unnecessary. A similar experiment has been performed by Carpenter and Wilson[2] at 143 MeV.

The experiment itself is standard in design. Plan and elevation views are shown in Fig. 1. A transversely polarized proton beam is directed onto the target, and neutrons recoiling in a plane perpendicular to the incident polarization are detected in a scintillation telescope. Under these conditions the measured asymmetry e is related to the beam polarization P_b and the reaction asymmetry P by the relation $e=PP_b$. As P_b and e are measured, P can be found.

II. APPARATUS AND PROCEDURE

The Beam

The polarized proton beam of the Rochester synchrocyclotron was stochastically accelerated[3] with a duty cycle of approximately 30%. Mean energy, polarization, and other beam parameters are listed in Table I. After

* Work supported by the U. S. Atomic Energy Commission.
† Submitted by one of us (D. Spalding) in partial fulfillment of the requirements for the Ph. D. degree in physics at the University of Rochester, Rochester, New York.
[1] N. W. Reay, E. H. Thorndike, D. Spalding, and A. R. Thomas, preceding paper, Phys. Rev. **150**, 801 (1966).
[2] S. G. Carpenter and R. Wilson, Phys. Rev. **113**, 650 (1959).
[3] E. Nordberg, IEEE Trans. Nucl. Sci. **NS-12**, 973 (1965).